SearchPath

Documentation

Author: Felix Meier

Version: 1.0

Date: May 17, 2021

File: SearchPath_Documentation_EN_US_Letter.docx

Felix Meier
+41 44 867 3723

Roggenfarstrasse 31
www.felmeier.com

CH – 8193 Eglisau
felix.meier.45@bluewin.ch

Contents

Felix Meier
+41 44 867 3723
Roggenfarstrasse 31
www.felmeier.com
CH – 8193 Eglisau
felix.meier.45@bluewin.ch

1 Introduction

The project is to provide a means for the examination of the direction of the field lines and of the relative field strength at the location of a receiver at any point in the surroundings of a magnetic dipole buried in snow. In particular, this location would be on the plane where a transceiver in search mode would be operated by some user.

1.1 Setup

For the environment, we use a 5 layer model:

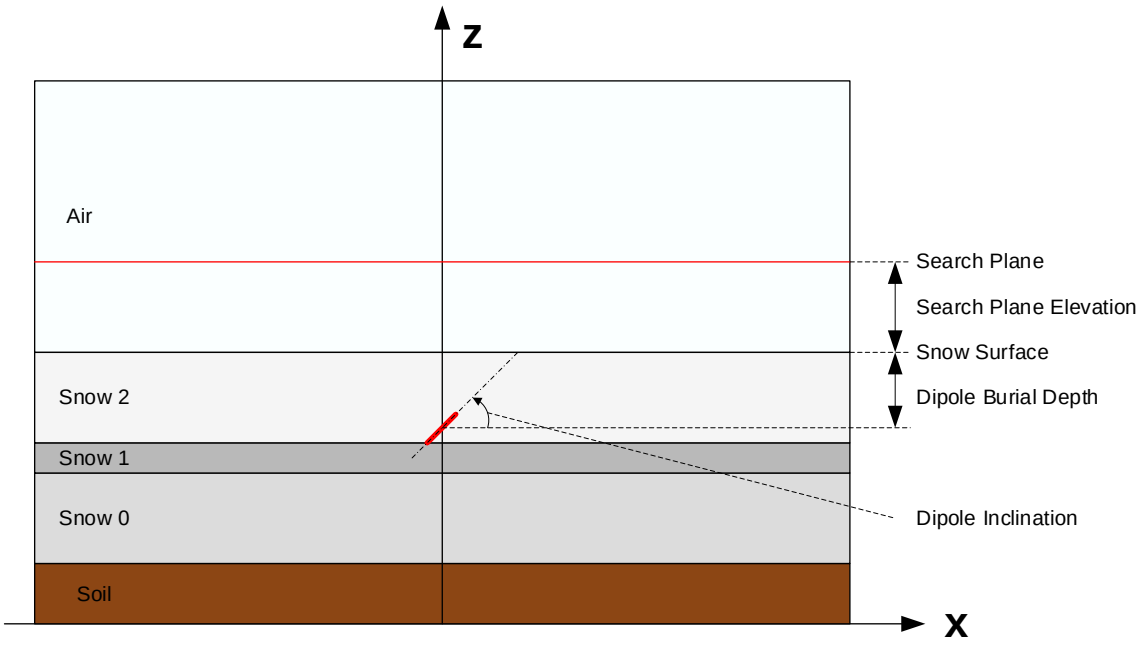

The bottom layer is made of soil. Above the soil, up to three layers of snow with different properties may be specified. On the top, there is an air layer. The individual layers are assumed to be homogenous, i.e. their permeability, permittivity and conductivity will be constant within the layer.

The dipole may be positioned anywhere within one of the snow layers. Its inclination may vary from 0° to 90°. The dipole is always centered on the x and y axes of the area under consideration.

The search plane is where the searching transceiver would be operated. It may be located at any elevation between the snow surface and the top of the air layer.

Felix Meier
+41 44 867 3723
Roggenfarstrasse 31
www.felmeier.com
CH – 8193 Eglisau
felix.meier.45@bluewin.ch

The space of interest is a rectangular block:

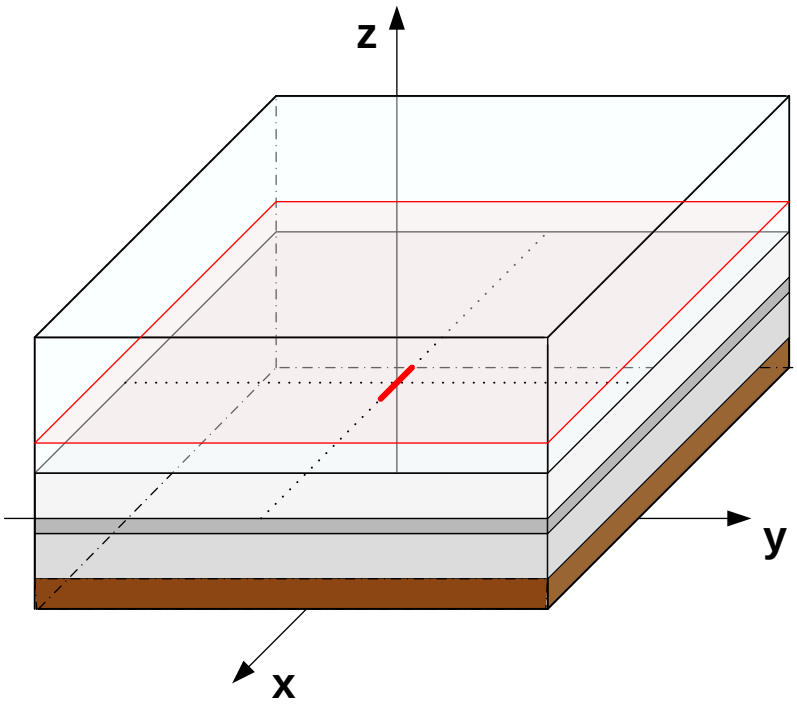

The default block dimensions are 20 meters by 20 meters by 10 meters. The above example shows a transceiver buried at the bottom of the topmost snow layer. The inclination of the transceiver antenna relative to the x axis is 0°. The search plane (red) would typically be about 80 centimeters above the snow surface.

There are no closed form solutions for the electromagnetic field in an inhomogeneous space. To solve our problem, we therefore resort to the FDTD (Finite Difference Time Domain) algorithm for numerical integration of the Maxwell differential equations within the space of interest. This method was originally proposed by Yee [102] and is treated in detail by Taflove and Hagness in [100].

The space of interest is divided into cubes with an edge length of 10 cm (default). The six update equations for each cube need to be calculated between 300 and 1'000 times, depending on the electromagnetic properties of the individual layers. So do not expect an immediate result when calculating a specific configuration. The calculation will take one to several minutes on a fast PC to complete.

Felix Meier
+41 44 867 3723
Roggenfarstrasse 31
www.felmeier.com
CH – 8193 Eglisau
felix.meier.45@bluewin.ch

2 Finite Difference Time Domain (FDTD) Analysis

For an introduction to the FDTD algorithm, see Taflove and Hagness [100]. In this text, we only go into detail about the project-specific items that deviate from the generalized theory.

2.1 The Coordinate System

2.1.1 The Yee Cells

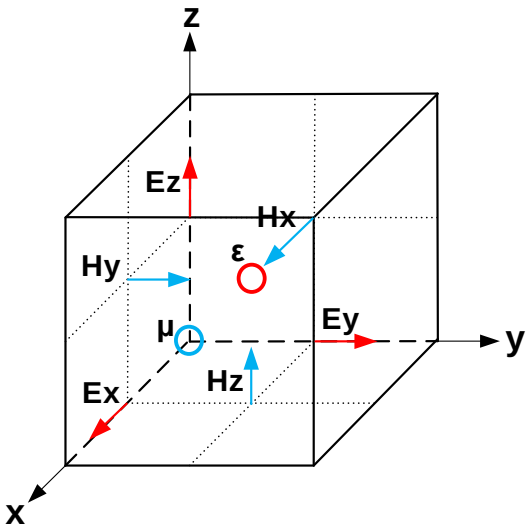

Fig. 1

All cell edges are of equal length. The permittivity ε is defined at the center of the cell. The permeability μ is defined at the corner that is closest to the origin of the coordinate system.

In the reference [100], the E and H vectors are interchanged. We use the above definitions, since they are also used in the original paper by Yee [102] and in the papers by Schneider [108] and Neva [107].

2.1.2 The Full Space

The full space under investigation is made of X by Y by Z Yee cells. Since we will be using spatial derivatives of the H field at the root of the E field vectors, and spatial derivatives of the E field at the root of the H field vectors, we obviously need one extra cell in each dimension. As a consequence, the first valid vectors for the individual field components will be

Ex: [0,1,1]	Ey: [1,0,1]	Ez: [1,1,0]
Hx: [0,0,0]	Hy: [0,0,0]	Hz: [0,0,0]

And the last valid vectors at the corner of the space that is opposite the origin will be

Ex: [X-1,Y,Z]	Ey: [X,Y-1,Z]	Ez: [X,Y,Z-1]
Hx: [X,Y-1, Z-1]	Hy: [X-1,Y, Z-1]	Hz: [X-1,Y-1, Z]

For the space walls, we use the following notation:

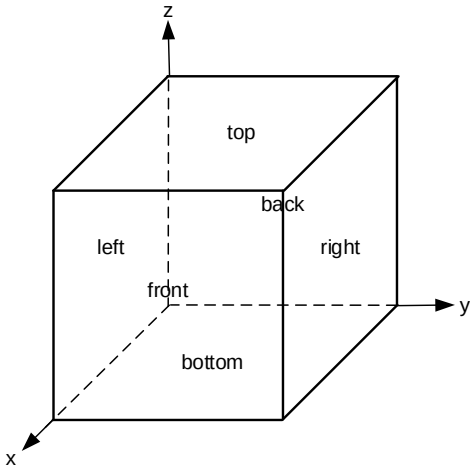

In order to be able to place the magnetic dipole exactly at the center of the space in an x/y plane, we will use odd numbers for X, Y and Z.

2.1.3 Layer Properties

In order to use the permittivity and the permeability at the root of the vector to be calculated, we use the average of the four neighboring values in the plane that is normal to the vector and contains the root of the vector. Since all layer interfaces will be in an x/y plane, this averaging will only need to be done for a single layer of cells at the layer interface.

2.2 The Algorithm

2.2.1 The Maxwell Equations

$$\frac{\partial \vec{\mathrm{E}}}{\partial \mathrm{t}} = -\frac{\sigma}{\varepsilon}\vec{\mathrm{E}} + \frac{1}{\varepsilon}(\nabla \times \vec{\mathrm{H}}) - \frac{1}{\varepsilon}\vec{\mathrm{J}}_{\mathrm{s}} \tag{201}$$

$$\frac{\partial \vec{\mathrm{H}}}{\partial \mathrm{t}} = -\frac{\sigma_{\mathrm{m}}}{\mu}\vec{\mathrm{H}} - \frac{1}{\mu}(\nabla \times \vec{\mathrm{E}}) - \frac{1}{\mu}\vec{\mathrm{J}}_{\mathrm{ms}} \tag{202}$$

Where

σ is the electric conductivity

σ_m is the equivalent magnetic loss

$\frac{\sigma}{\varepsilon}\vec{E}$ is the electric conduction current

$\vec{J}_S$ is the electric current density

$\frac{\sigma_m}{\mu}\vec{H}$ is the magnetic conduction current

$\vec{J}_{ms}$ is the magnetic current density

2.2.2 The Update Equations

Unwinding the curl operators, we get

$$\frac{\partial \vec{\mathrm{E}}}{\partial \mathrm{t}} = -\frac{\sigma}{\varepsilon}\vec{\mathrm{E}} + \frac{1}{\varepsilon}\left[a_x\left(\frac{\partial \mathrm{H_z}}{\partial \mathrm{y}} - \frac{\partial \mathrm{H_y}}{\partial \mathrm{z}}\right) + a_y\left(\frac{\partial \mathrm{H_x}}{\partial \mathrm{z}} - \frac{\partial \mathrm{H_z}}{\partial \mathrm{x}}\right) + a_z\left(\frac{\partial \mathrm{H_y}}{\partial \mathrm{x}} - \frac{\partial \mathrm{H_x}}{\partial \mathrm{y}}\right)\right] - \frac{1}{\varepsilon}\vec{\mathrm{J}}_{\mathrm{s}} \tag{203}$$

$$\frac{\partial \vec{\mathrm{H}}}{\partial \mathrm{t}} = -\frac{\sigma_{\mathrm{m}}}{\mu}\vec{\mathrm{H}} + \frac{1}{\mu}\left[a_x\left(\frac{\partial \mathrm{E_y}}{\partial \mathrm{z}} - \frac{\partial \mathrm{E_z}}{\partial \mathrm{y}}\right) + a_y\left(\frac{\partial \mathrm{E_z}}{\partial \mathrm{x}} - \frac{\partial \mathrm{E_x}}{\partial \mathrm{z}}\right) + a_z\left(\frac{\partial \mathrm{E_x}}{\partial \mathrm{y}} - \frac{\partial \mathrm{E_y}}{\partial \mathrm{x}}\right)\right] - \frac{1}{\mu}\vec{\mathrm{J}}_{\mathrm{ms}} \tag{204}$$

Where the a_i are the unit vectors of the three dimensional cartesian coordinate system.

Noting that each iteration of the loop through all x, y, and z index values actually consists of two steps, namely updating the E field components and then the H field components, and those two steps may be looked at as single step consisting of two half steps, we get the following equations:

$$\vec{\mathrm{E}}_{\mathrm{n}} = \frac{1-\frac{\Delta \mathrm{t}\bullet\sigma}{2\varepsilon}}{1+\frac{\Delta \mathrm{t}\bullet\sigma}{2\varepsilon}}\vec{\mathrm{E}}_{\mathrm{n-1}} + \frac{\frac{\Delta \mathrm{t}}{\varepsilon}}{1+\frac{\Delta \mathrm{t}\bullet\sigma}{2\varepsilon}}\left[a_x\left(\frac{\partial \mathrm{H_z}}{\partial \mathrm{y}} - \frac{\partial \mathrm{H_y}}{\partial \mathrm{z}}\right) + a_y\left(\frac{\partial \mathrm{H_x}}{\partial \mathrm{z}} - \frac{\partial \mathrm{H_z}}{\partial \mathrm{x}}\right) + a_z\left(\frac{\partial \mathrm{H_y}}{\partial \mathrm{x}} - \frac{\partial \mathrm{H_x}}{\partial \mathrm{y}}\right)\right] \tag{205}$$

Where the H derivatives are taken at time n-1/2 and

$$\vec{\mathrm{H}}_{\mathrm{n+1/2}} = \frac{1-\frac{\Delta \mathrm{t}\bullet\sigma_{\mathrm{m}}}{2\mu}}{1+\frac{\Delta \mathrm{t}\bullet\sigma_{\mathrm{m}}}{2\mu}}\vec{\mathrm{H}}_{\mathrm{n-1/2}} + \frac{\frac{\Delta \mathrm{t}}{\mu}}{1+\frac{\Delta \mathrm{t}\bullet\sigma_{\mathrm{m}}}{2\mu}}\left[a_x\left(\frac{\partial \mathrm{E_y}}{\partial \mathrm{z}} - \frac{\partial \mathrm{E_z}}{\partial \mathrm{y}}\right) + a_y\left(\frac{\partial \mathrm{E_z}}{\partial \mathrm{x}} - \frac{\partial \mathrm{E_x}}{\partial \mathrm{z}}\right) + a_z\left(\frac{\partial \mathrm{E_x}}{\partial \mathrm{y}} - \frac{\partial \mathrm{E_y}}{\partial \mathrm{x}}\right)\right] \tag{206}$$

Where the E derivatives are taken at time n.

Note that we have suppressed the current densities, since we will take care of them when inserting the dipole into some layer by jamming some edges of the central cell.

The coefficients are assumed to be constant in time, but they will be different for every direction and for every layer in our model. For simplifying the notation, we will use the following assignments:

$$\frac{1-\frac{\Delta t \bullet \sigma_x}{2\varepsilon_x}}{1+\frac{\Delta t \bullet \sigma_x}{2\varepsilon_x}} = \mathrm{UcEx}_{[0]} \qquad \frac{\frac{\Delta t}{\varepsilon_x}}{1+\frac{\Delta t \bullet \sigma_x}{2\varepsilon_x}} = \mathrm{UcEx}_{[1]} \tag{207}$$

$$\frac{1-\frac{\Delta t \bullet \sigma_{mx}}{2\mu_x}}{1+\frac{\Delta t \bullet \sigma_{mx}}{2\mu_x}} = \mathrm{UcHx}_{[0]} \qquad \frac{\frac{\Delta t}{\mu_x}}{1+\frac{\Delta t \bullet \sigma_{mx}}{2\mu_x}} = \mathrm{UcHx}_{[1]} \tag{208}$$

and so forth for the other dimensions.

For the effective update coefficients, we use the following formulas:

$$\frac{1-\frac{\Delta t \bullet \sigma_x}{2\varepsilon_x}}{1+\frac{\Delta t \bullet \sigma_x}{2\varepsilon_x}} = \mathrm{UcEx}_{[0]} \qquad \frac{\frac{\Delta t}{\varepsilon_x \bullet \Delta}}{1+\frac{\Delta t \bullet \sigma_x}{2\varepsilon_x}} = \mathrm{UcEx}_{[1]} \tag{209}$$

$$\frac{1-\frac{\Delta t \bullet \sigma_{mx}}{2\mu_x}}{1+\frac{\Delta t \bullet \sigma_{mx}}{2\mu_x}} = \mathrm{UcHx}_{[0]} \qquad \frac{\frac{\Delta t}{\mu_x \bullet \Delta}}{1+\frac{\Delta t \bullet \sigma_{mx}}{2\mu_x}} = \mathrm{UcHx}_{[1]} \tag{210}$$

where Δ is the edge length of the Yee cells, since all edges are of equal length. The formulas for the y and z components of the update coefficients are analogous.

By replacing the derivatives by finite differences, the discrete update equations become (see Neva [107] section 3.2, or Schneider [108], section 3.6.2):

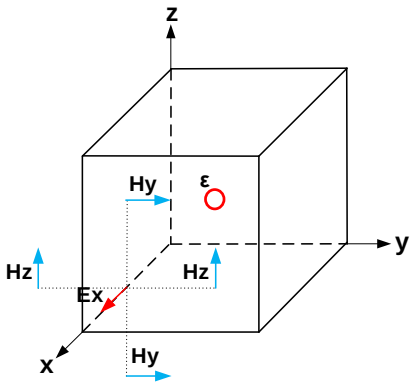

$$\mathrm{Ex}^{n}_{[i,j,k]} = \mathrm{UcEx}_{[0]} \cdot \mathrm{Ex}^{n-1}_{[i,j,k]} + \mathrm{UcEx}_{[1]}\left\{\left(\mathrm{Hz}_{[i,j,k]} - \mathrm{Hz}_{[i,j-1,k]}\right) - \left(\mathrm{Hy}_{[i,j,k]} - \mathrm{Hy}_{[i,j,k-1]}\right)\right\} \quad (211)$$

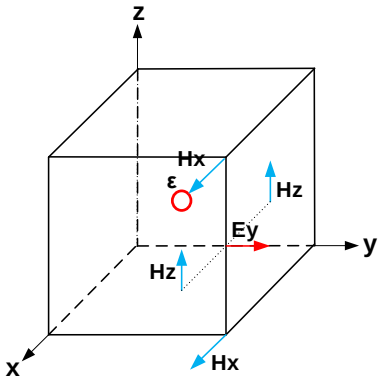

$$\mathrm{Ey}^{n}_{[i,j,k]} = \mathrm{UcEy}_{[0]} \cdot \mathrm{Ey}^{n-1}_{[i,j,k]} + \mathrm{UcEy}_{[1]}\left\{\left(\mathrm{Hx}_{[i,j,k]} - \mathrm{Hx}_{[i,j,k-1]}\right) - \left(\mathrm{Hz}_{[i,j,k]} - \mathrm{Hz}_{[i-1,j,k]}\right)\right\} \quad (212)$$

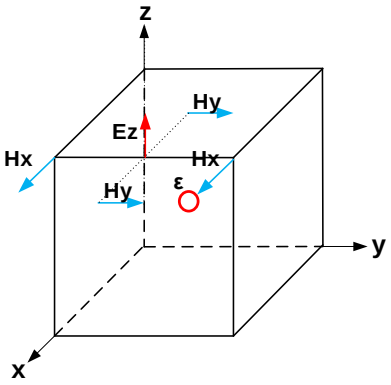

$$\mathrm{Ez}^{n}_{[i,j,k]} = \mathrm{UcEz}_{[0]} \cdot \mathrm{Ez}^{n-1}_{[i,j,k]} + \mathrm{UcEz}_{[1]}\left\{\left(\mathrm{Hy}_{[i,j,k]} - \mathrm{Hy}_{[i-1,j,k]}\right) - \left(\mathrm{Hx}_{[i,j,k]} - \mathrm{Hx}_{[i,j-1,k]}\right)\right\} \quad (213)$$

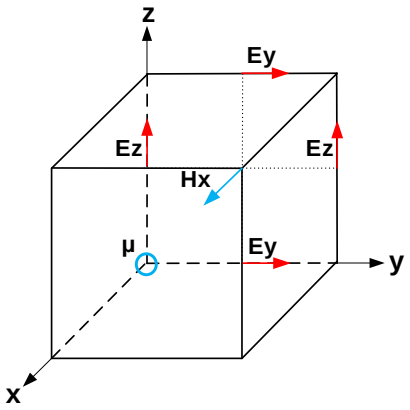

$$Hx^{n}_{[i,j,k]} = UcHx_{[0]} \cdot Hx^{n-1}_{[i,j,k]} + UcHx_{[1]}\{(Ey_{[i,j,k+1]} - Ey_{[i,j,k]}) - (Ez_{[i,j+1,k]} - Ez_{[i,j,k]})\} \quad (214)$$

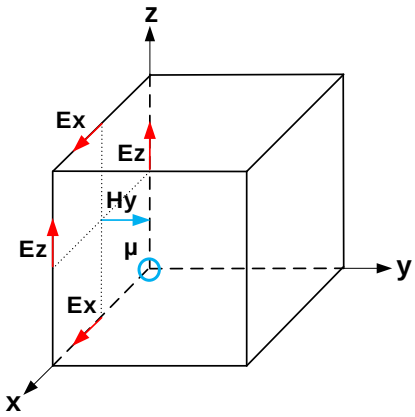

$$Hy^{n}_{[i,j,k]} = UcHy_{[0]} \cdot Hy^{n-1}_{[i,j,k]} + UcHy_{[1]}\{(Ez_{[i+1,j,k]} - Ez_{[i,j,k]}) - (Ex_{[i,j,k+1]} - Ex_{[i,j,k]})\} \quad (215)$$

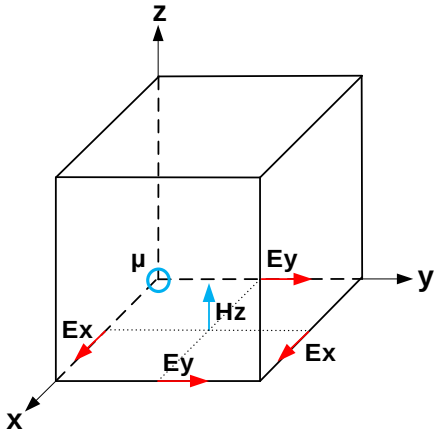

$$Hz^{n}_{[i,j,k]} = UcHz_{[0]} \cdot Hz^{n-1}_{[i,j,k]} + UcHz_{[1]}\{(Ex_{[i,j+1,k]} - Ex_{[i,j,k]}) - (Ey_{[i+1,j,k]} - Ey_{[i,j,k]})\} \quad (216)$$

Felix Meier
+41 44 867 3723
Roggenfarstrasse 31
www.felmeier.com
CH – 8193 Eglisau
felix.meier.45@bluewin.ch

2.2.3 The Material Properties

For the effective material properties, we use the following formulas:

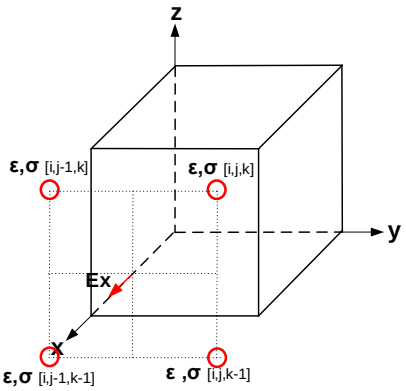

$$\varepsilon x, \sigma x_{[i,j,k]} = \left\{\varepsilon, \sigma_{[i,j,k]} + \varepsilon, \sigma_{[i,j-1,k]} + \varepsilon, \sigma_{[i,j-1,k-1]} + \varepsilon, \sigma_{[i,j,k-1]}\right\} / 4 \quad (217)$$

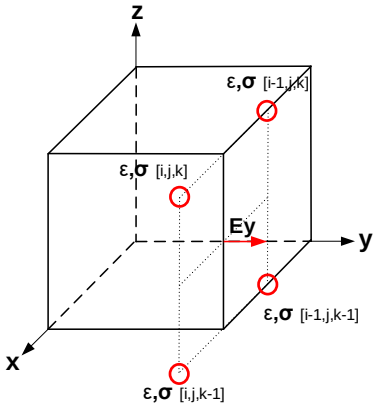

$$\varepsilon y, \sigma y_{[i,j,k]} = \left\{\varepsilon, \sigma_{[i,j,k]} + \varepsilon, \sigma_{[i-1,j,k]} + \varepsilon, \sigma_{[i-1,j,k-1]} + \varepsilon, \sigma_{[i,j,k-1]}\right\} / 4 \quad (218)$$

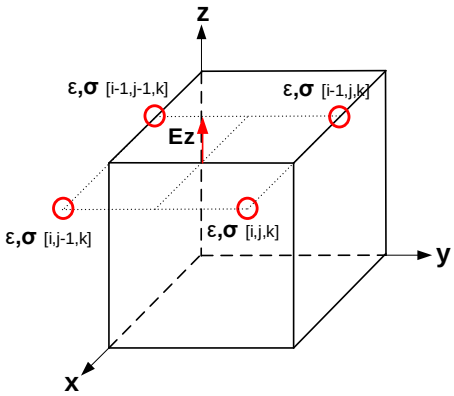

$$\varepsilon z, \sigma z_{[i,j,k]} = \left\{\varepsilon, \sigma_{[i,j,k]} + \varepsilon, \sigma_{[i-1,j,k]} + \varepsilon, \sigma_{[i-1,j-1,k]} + \varepsilon, \sigma_{[i,j-1,k]}\right\} / 4 \quad (219)$$

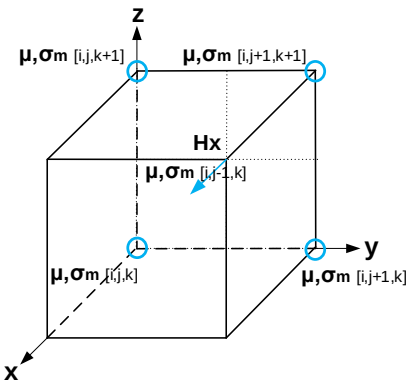

$$\mu x, \sigma_m x_{[i,j,k]} = \left\{\mu, \sigma_{m\,[i,j,k]} + \mu, \sigma_{m\,[i,j+1,k]} + \mu, \sigma_{m\,[i,j+1,k+1]} + \mu, \sigma_{m\,[i,j,k+1]}\right\} / 4 \qquad (220)$$

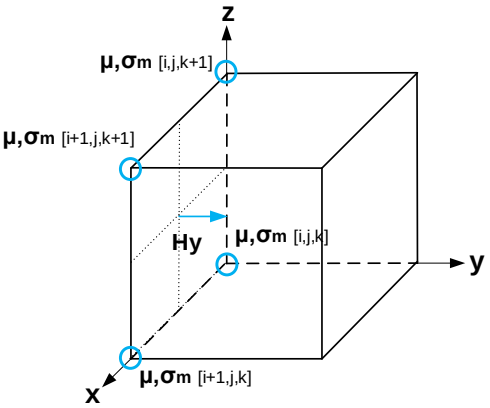

$$\mu y, \sigma_m y_{[i,j,k]} = \left\{\mu, \sigma_{m\,[i,j,k]} + \mu, \sigma_{m\,[i+1,j,k]} + \mu, \sigma_{m\,[i+1,j,k+1]} + \mu, \sigma_{m\,[i,j,k+1]}\right\} / 4 \qquad (221)$$

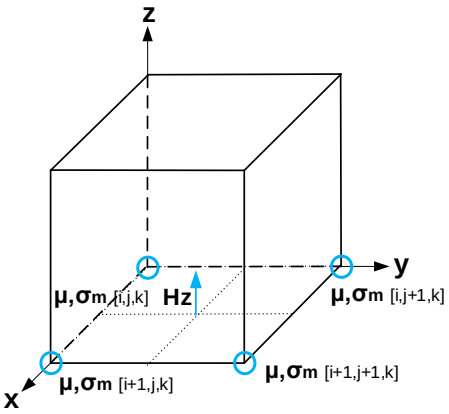

$$\mu z, \sigma_m z_{[i,j,k]} = \left\{\mu, \sigma_{m\,[i,j,k]} + \mu, \sigma_{m\,[i+1,j,k]} + \mu, \sigma_{m\,[i+1,j,k+1]} + \mu, \sigma_{m\,[i,j+1,k]}\right\} / 4 \qquad (222)$$

Because all layer interfaces are in an x-y plane, the $UcEz_{[]}$ and $UcHz_{[]}$ will always be depending on $\varepsilon_{[i,j,k]}$, $\sigma_{[i,j,k]}$, $\mu_{[i,j,k]}$, $\sigma_{m[i,j,k]}$ only. The same goes for the $UcEx_{[]}$, $UcHx_{[]}$, $UcEy_{[]}$ and $UcHy_{[]}$ within the individual layers. But there are exceptions to this rule:

For the $UcEx_{[]}$ and $UcEy_{[]}$ of the bottom cells of every layer, the averages as per the above formulas should be used. For the bottom cells of the bottom layer (i.e. the soil layer), we will assume that the layer below exhibits the same material properties.

For the $UcHx_{[]}$ and $UcHy_{[]}$ of the top cells of every layer, the averages as per the above formulas should be used. For the top cells of the top layer (i.e. the air layer), we will assume that the layer above exhibits the same material properties.

2.3 The Maximum Time Step

The maximum time step is given by (see [101], formula (7))

$$\Delta t \leq \frac{1}{v_{max} \cdot \sqrt{\frac{1}{\Delta x^2}+\frac{1}{\Delta y^2}+\frac{1}{\Delta z^2}}} \tag{300}$$

For equal Δ in all 3 dimensions, this becomes

$$\Delta t \leq \frac{1}{v_{max} \cdot \sqrt{\frac{3}{\Delta^2}}} = \frac{\Delta}{v_{max} \bullet \sqrt{3}} \tag{301}$$

or, as a rule of thumb:

$$\Delta t \leq \frac{\Delta}{2 \cdot v_{max}} \tag{302}$$

Where v_{max} stands for the group velocity and the speed of light is a worst case value. Remember: the layer with the maximum propagation speed is the air layer, where v_{max} is equal to the speed of light.

The basic idea behind this is that the wavefront should not propagate beyond one grid interval within one time step. The maximum time step ensures that the integration of the partial difference equations will produce correct results. This rule is the Courant-Friedrichs-Lewy criterion, see [104].

2.4 The Number of Integration Steps

The number of integration steps must be sufficient for the signal from the source (the dipole) to reach the boundaries of the space under investigation.

For the number of time steps, we must make sure that the propagating signals reach the points in the space under investigation that are the most distant from the source of the signal. The signal source will always be centered within the x and y dimensions, and we assume that the signal source will be about at the center of the z dimension. So the maximum distance to reach a corner of the space becomes

$$d = \sqrt{\left(\frac{N_x}{2}\right)^2 + \left(\frac{N_y}{2}\right)^2 + \left(\frac{N_z}{2}\right)^2} \cdot \Delta = \frac{1}{2}\sqrt{N_x^2 + N_y^2 + N_z^2} \cdot \Delta \quad (400)$$

where N_z is double the longer of the distances from the dipole to the top or bottom face.

The soil will be the medium with the lowest propagation speed. The propagation speed in soil will be

$$v_{soil} = \frac{1}{\sqrt{\mu_0 \cdot \mu_r \cdot \varepsilon_0 \cdot \epsilon_r}} = c \cdot \frac{1}{\sqrt{\mu_r \cdot \epsilon_r}} \quad (401)$$

Applying the soil speed over the entire distance would result in a high number of steps. A more economic approach is to limit the increase in steps to the part of the path that lies inside the soil layer. So we define the ratio of the surface height of the soil to the height of the dipole (both measured from the bottom face of the space under investigation):

$$r_{Soil} = \frac{h_{Soil}}{h_{Dipole}}$$

For the signals to reach the corners, the minimum time required will then become

$$t_{min} = \frac{d}{v_{soil}} \cdot r_{Soil} + \frac{d}{c} \cdot (1 - r_{Soil})$$

And the number of time steps becomes

$$\text{TimeSteps} = \frac{t_{min}}{\Delta t} \quad (403)$$

Inserting realistic values for soil, we get

$$\varepsilon_r = 8 \quad \sigma = 1e-4 \quad \omega = 2\pi \cdot 457e+3 \qquad |\varepsilon| = \sqrt{\varepsilon_r^2 \cdot \frac{\sigma}{\omega \bullet \varepsilon_0}} = 8.914 \approx 9.0$$

With a height ratio r_{soil} of 0.4, this results in an increase in the number of steps by a factor of about 1.8.

If the number of integration steps is very large, i. e. > 600, there will be a remarkable effect of the reflections, in particular at the top face of the air layer.

Felix Meier
+41 44 867 3723
Roggenfarstrasse 31
www.felmeier.com
CH – 8193 Eglisau
felix.meier.45@bluewin.ch

2.5 Initial Conditions

At the onset, all field values of all cells are set to 0.0e+0. The excitation currents for the dipole start with $A_0 \cdot \sin(\omega \cdot n \cdot \Delta t)$, n = 0. At 600 steps, the sine will become about 0.28.

2.6 Steady State

In order to reach steady state, the number of steps would have to include several periods of the excitation signal. At 457 kHz, this would mean that the integration would have to go up to n times

(one period / time step) = (1 / (1.667e-10 · 457e+3)) = 13'126

steps, so this would be extremely time consuming, and reflections would prevail. For this reason, the E and H field values are only to be used as relative values. This is of no significance to our application, since we are primarily interested in the direction of the field lines and not in their magnitude.

Felix Meier
+41 44 867 3723
Roggenfarstrasse 31
www.felmeier.com
CH – 8193 Eglisau
felix.meier.45@bluewin.ch

2.7 The Dipole

The dipole antenna will be centered within the x-y plane. Its axis will be located in the x-z plane. The inclination φ will be relative to the x axis:

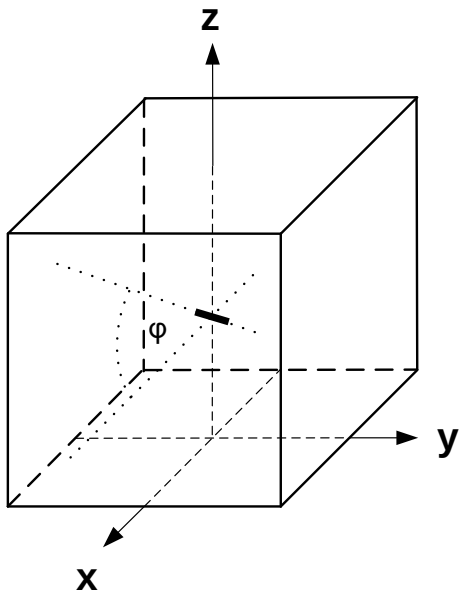

The field generated by the dipole in each axis will be simulated by two pairs of loop currents that circulate in the faces that are normal to the respective axis:

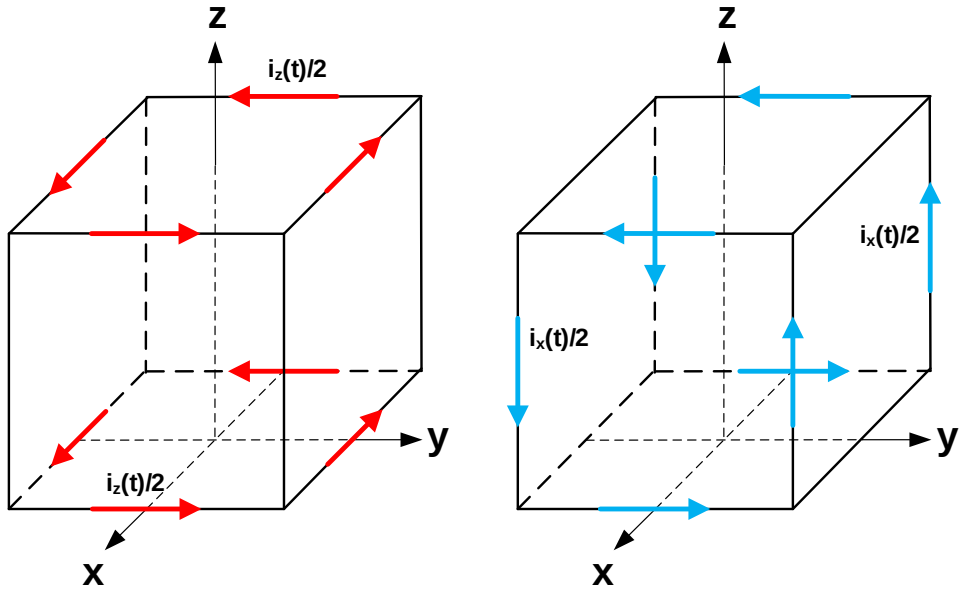

As explained in [106], section 3.3, this is easily implemented by introducing the excitation current terms into the standard update equations for the electric field.

$$\vec{E}_n = \frac{1-\frac{\Delta t \cdot \sigma}{2\varepsilon}}{1+\frac{\Delta t \cdot \sigma}{2\varepsilon}}\vec{E}_{n-1} + \frac{\frac{\Delta t}{\varepsilon}}{1+\frac{\Delta t \cdot \sigma}{2\varepsilon}}\left[a_x\left(\frac{\partial H_z}{\partial y}-\frac{\partial H_y}{\partial z}\right)+a_y\left(\frac{\partial H_x}{\partial z}-\frac{\partial H_z}{\partial x}\right)+a_z\left(\frac{\partial H_y}{\partial x}-\frac{\partial H_x}{\partial y}\right)-\vec{J}_s\right] \quad (500)$$

Since we optimized out the cell edge length and made it part of the update coefficients (see (209, 210), (211) must be changed to

$$Ex^n_{[i,j,k]} = UcEx_{[0]} \cdot Ex^{n-1}_{[i,j,k]} + UcEx_{[1]} \cdot \left\{\left(Hz_{[i,j,k]} - Hz_{[i,j-1,k]}\right) - \left(Hy_{[i,j,k]} - Hy_{[i,j,k-1]}\right) - \Delta \cdot J_s\right\} \quad (501)$$

where J_s is the electric current density in A/m²:

$$J_s(t) = \frac{i(t)}{\Delta^2} \quad (502)$$

Obviously, analog changes must be applied to (212) and (213). So, after the update equations have been done:

$$\vec{E}^n_{[i,j,k]} = \vec{E}^n_{[i,j,k]} - \overrightarrow{UcEx_{[1]_{[\iota,J,k]}}} \cdot \Delta \cdot \vec{J_s} \quad (503)$$

The H field strength at the center of a square current loop with edge length Δ is

$$H = I_0 \cdot \frac{2\sqrt{2}}{\Delta \cdot \pi} \quad (504)$$

so

$$I_0 = \frac{\Delta \cdot \pi \cdot H}{2\sqrt{2}} \quad (505)$$

A decent avalanche transceiver transmits at a field strength of about H_0 = 2 mA/m at a distance of 1 m on the main axis of the dipole. Since the near field strength is inversely proportional to the third power of the distance from the dipole, the field strength H at a distance Δ/2 must be

$$H == H_0 \cdot \frac{1}{\left(\frac{\Delta}{2}\right)^3} = H_0 \cdot \frac{2^3}{\Delta^3} = H_0 \cdot \frac{8}{\Delta^3} \quad (506)$$

As a consequence

$$I_0 = H_0 \cdot \frac{8 \cdot \Delta \cdot \pi}{\Delta^3 \cdot 2\sqrt{2}} = H_0 \bullet \frac{4 \cdot \pi}{\Delta^2 \cdot \sqrt{2}} \quad (507)$$

and

$$J_s(t) = \frac{1}{\Delta^2} \cdot I_0 \cdot \cos(\omega t) = H_0 \cdot \frac{4 \cdot \pi}{\Delta^4 \cdot \sqrt{2}} \cdot \cos(\omega t) \quad (508)$$

So the vectorized update equation (503) becomes

$$\vec{E}^{n}_{[i,j,k]} = \vec{E}^{n}_{[i,j,k]} - Uc\overrightarrow{E_{[1]_{[\iota,J,k]}}} \cdot \vec{H_0} \cdot \frac{4\cdot\pi}{\Delta^3\cdot\sqrt{2}} \bullet \cos(\omega t) \tag{509}$$

The update equations for the 12 edges that are affected are then

$$Ex_{[i,j,k]} = Ex_{[i,j,k]} - UcEx_{[1]} \cdot \frac{1}{2\cdot\Delta}\left[+i_z(t) - i_y(t)\right] \tag{510}$$
$$Ey_{[i,j,k]} = Ey_{[i,j,k]} - UcEy_{[1]} \cdot \frac{1}{2\cdot\Delta}\left[-i_z(t)\right] \tag{511}$$
$$Ez_{[i,j,k]} = Ez_{[i,j,k]} - UcEz_{[1]} \cdot \frac{1}{2\cdot\Delta}\left[+i_y(t)\right] \tag{512}$$

$$Ex_{[i,j+1,k]} = Ex_{[i,j+1,k]} - UcEx_{[1]} \cdot \frac{1}{2\cdot\Delta}\left[-i_z(t) - i_y(t)\right] \tag{513}$$
$$Ez_{[i,j+1,k]} = Ez_{[i,j+1,k]} - UcEz_{[1]} \cdot \frac{1}{2\cdot\Delta}\left[+i_y(t)\right] \tag{514}$$

$$Ey_{[i+1,j,k]} = Ey_{[i+1,j,k]} - UcEy_{[1]} \cdot \frac{1}{2\cdot\Delta}\left[+i_z(t)\right] \tag{515}$$
$$Ez_{[i+1,j,k]} = Ez_{[i+1,j,k]} - UcEz_{[1]} \cdot \frac{1}{2\cdot\Delta}\left[-i_y(t)\right] \tag{516}$$

$$Ez_{[i+1,j+1,k]} = Ez_{[i+1,j+1,k]} - UcEz_{[1]} \cdot \frac{1}{2\cdot\Delta}\left[-i_y(t)\right] \tag{517}$$

$$Ex_{[i,j,k+1]} = Ex_{[i,j,k+1]} - UcEx_{[1]} \cdot \frac{1}{2\cdot\Delta}\left[+i_z(t) + i_y(t)\right] \tag{518}$$
$$Ey_{[i,j,k+1]} = Ey_{[i,j,k+1]} - UcEy_{[1]} \cdot \frac{1}{2\cdot\Delta}\left[-i_z(t)\right] \tag{519}$$

$$Ex_{[i,j+1,k+1]} = Ex_{[i,j+1,k+1]} - UcEx_{[1]} \cdot \frac{1}{2\cdot\Delta}\left[-i_z(t) + i_y(t)\right] \tag{520}$$

$$Ey_{[i+1,j,k+1]} = Ey_{[i+1,j,k+1]} - UcEy_{[1]} \cdot \frac{1}{2\cdot\Delta}\left[+i_z(t)\right] \tag{521}$$

where

$$i_y(t) = I_0 \cdot \cos(\omega t) \cdot \cos(\varphi) \tag{522}$$

$$i_z(t) = I_0 \cdot \cos(\omega t) \cdot \sin(\varphi) \tag{523}$$

Note that, since we want the dipole to be centered within a cell, we will have two loop currents on opposite faces of the cell, so the loop current must be divided by 2.

Unfortunately, using the above type of dipole excitation requires a very large number of integration steps before the numerical values of the H field in the individual cells become suitable for making nice field line curves. The calculation of a particular configuration takes a lot of time, and the effects of reflections on the faces become much more important.

To mitigate these effects, we therefore jam the dipole excitation currents, not making use of the previous E field values in the excited cells:

$$\mathrm{Ex}_{[i,j,k]} = \mathrm{UcEx}_{[1]} \cdot \frac{1}{2\cdot\Delta}\left[+i_z(t) - i_y(t)\right] \quad (523)$$

$$\mathrm{Ey}_{[i,j,k]} = \mathrm{UcEy}_{[1]} \cdot \frac{1}{2\cdot\Delta}\left[-i_z(t)\right] \quad (525)$$

$$\mathrm{Ez}_{[i,j,k]} = \mathrm{UcEz}_{[1]} \cdot \frac{1}{2\cdot\Delta}\left[+i_y(t)\right] \quad (526)$$

$$\mathrm{Ex}_{[i,j+1,k]} = \mathrm{UcEx}_{[1]} \cdot \frac{1}{2\cdot\Delta}\left[-i_z(t) - i_y(t)\right] \quad (527)$$

$$\mathrm{Ez}_{[i,j+1,k]} = \mathrm{UcEz}_{[1]} \cdot \frac{1}{2\cdot\Delta}\left[+i_y(t)\right] \quad (526)$$

$$\mathrm{Ey}_{[i+1,j,k]} = \mathrm{UcEy}_{[1]} \cdot \frac{1}{2\cdot\Delta}\left[+i_z(t)\right] \quad (529)$$

$$\mathrm{Ez}_{[i+1,j,k]} = \mathrm{UcEz}_{[1]} \cdot \frac{1}{2\cdot\Delta}\left[-i_y(t)\right] \quad (530)$$

$$\mathrm{Ez}_{[i+1,j+1,k]} = \mathrm{UcEz}_{[1]} \cdot \frac{1}{2\cdot\Delta}\left[-i_y(t)\right] \quad (531)$$

$$\mathrm{Ex}_{[i,j,k+1]} = \mathrm{UcEx}_{[1]} \cdot \frac{1}{2\cdot\Delta}\left[+i_z(t) + i_y(t)\right] \quad (532)$$

$$\mathrm{Ey}_{[i,j,k+1]} = \mathrm{UcEy}_{[1]} \cdot \frac{1}{2\cdot\Delta}\left[-i_z(t)\right] \quad (533)$$

$$\mathrm{Ex}_{[i,j+1,k+1]} = \mathrm{UcEx}_{[1]} \cdot \frac{1}{2\cdot\Delta}\left[-i_z(t) + i_y(t)\right] \quad (534)$$

$$\mathrm{Ey}_{[i+1,j,k+1]} = \mathrm{UcEy}_{[1]} \cdot \frac{1}{2\cdot\Delta}\left[+i_z(t)\right] \quad (535)$$

With this type of excitation, proper curve shapes are preserved, and the number of integration steps as outlined in section 2.4 produces good results without excessive effects due to reflections.

Felix Meier
+41 44 867 3723
Roggenfarstrasse 31
www.felmeier.com
CH – 8193 Eglisau
felix.meier.45@bluewin.ch

2.8 Absorbing Boundary Conditions

When simulating propagation in an infinite space within a limited space, some kind of absorption must be introduced on all faces of the limited space in order to minimize any reflections. Many different methods exist for this purpose, the most complex ones being the Perfect Matching Layer (PML) ones. Using perfect matching layers incurs much more complexity and computation time. For our purpose, the much simpler method proposed by Mur [103], enhanced by the superabsorption proposed by Mei and Fang [108] will do.

2.8.1 The Mur Absorbing Boundary Conditions

In his paper [103], Mur proposes a first order ABC (Absorbing Boundary Condition) and a second order ABC. The first order Mur ABC is easier to implement, although less accurate, and so we focus on that variant.

It is assumed that the direction of incidence of the waves onto the faces (boundaries) of the space is exactly parallel to the normal of the face and that the waves are exactly plane. The wave equation

$$\frac{\partial^2 W}{\partial t^2} = v_{max}^2 \cdot \left[\frac{\partial^2 W}{\partial x^2} + \frac{\partial^2 W}{\partial y^2} + \frac{\partial^2 W}{\partial z^2}\right] \tag{600}$$

at the individual faces can be written as

Rear face:

$$\frac{\partial E_z}{\partial t} = v_{rear} \cdot \frac{\partial E_z}{\partial x} \tag{601}$$

$$\frac{\partial E_y}{\partial t} = v_{rear} \cdot \frac{\partial E_y}{\partial x} \tag{602}$$

Front face:

$$\frac{\partial E_z}{\partial t} = -v_{front} \cdot \frac{\partial E_z}{\partial x} \tag{603}$$

$$\frac{\partial E_y}{\partial t} = -v_{front} \cdot \frac{\partial E_y}{\partial x} \tag{604}$$

Where

$$v_{front} = v_{rear} = \frac{c}{\sqrt{\mu_r \cdot \varepsilon_r}}$$

with analogous equations for the left, right, bottom and top faces.

Mur [108] suggests that the point in time and space where the finite differences are taken should be at an intermediate time between steps n and n+1 and at location Δ/2 from the boundary. So, when using central differences in both the space and time domains, (601) in discrete form will become

$$\frac{1}{2} \cdot \left[\frac{Ez_{0,j,k}^{n+1} - Ez_{0,j,k}^{n}}{\Delta t} + \frac{Ez_{1,j,k}^{n+1} - Ez_{1,j,k}^{n}}{\Delta t}\right] - v_{rear} \cdot \frac{1}{2} \cdot \left[\frac{Ez_{1,j,k}^{n+1} - Ez_{0,j,k}^{n+1}}{\Delta} + \frac{Ez_{1,j,k}^{n} - Ez_{0,j,k}^{n}}{\Delta}\right] = 0 \tag{605}$$

After some manipulations, we get

$$\mathrm{Ez}_{0,j,k}^{n+1} = \mathrm{Ez}_{1,j,k}^{n} + \frac{v_{rear} \bullet \Delta t - \Delta}{v_{rear} \bullet \Delta t + \Delta} \cdot \left[\mathrm{Ez}_{1,j,k}^{n+1} - \mathrm{Ez}_{0,j,k}^{n}\right] \tag{606}$$

For the front face, (603) becomes

$$\frac{1}{2} \cdot \left[\frac{\mathrm{Ez}_{N_x,j,k}^{n+1} - \mathrm{Ez}_{N_x,j,k}^{n}}{\Delta t} + \frac{\mathrm{Ez}_{N_x-1,j,k}^{n+1} - \mathrm{Ez}_{N_x-1,j,k}^{n}}{\Delta t}\right] + v_{front} \cdot \frac{1}{2} \cdot \left[\frac{\mathrm{Ez}_{N_x,j,k}^{n+1} - \mathrm{Ez}_{N_x-1,j,k}^{n+1}}{\Delta} + \frac{\mathrm{Ez}_{N_x,j,k}^{n} - \mathrm{Ez}_{N_x-1,j,k}^{n}}{\Delta}\right] = 0 \tag{607}$$

And (606) becomes

$$\mathrm{Ez}_{N_x,j,k}^{n+1} = \mathrm{Ez}_{N_x-1,j,k}^{n} + \frac{v_{front} \cdot \Delta t - \Delta}{v_{front} \cdot \Delta t + \Delta} \cdot \left[\mathrm{Ez}_{N_x-1,j,k}^{n+1} - \mathrm{Ez}_{N_x,j,k}^{n}\right] \tag{608}$$

To simplify the notation, we define the reflection coefficients

$$\mathrm{RC}_{i,j,k} = \frac{v_{i,j,k} \cdot \Delta t - \Delta}{v_{i,j,k} \cdot \Delta t + \Delta} \tag{609}$$

The update equations for all faces will then be:

Rear face:

$$\mathrm{Ey}_{0,j,k}^{n+1} = \mathrm{Ey}_{1,j,k}^{n} + \mathrm{RC}_{0,j,k} \cdot \left[\mathrm{Ey}_{1,j,k}^{n+1} - \mathrm{Ey}_{0,j,k}^{n}\right] \quad j: 0\ldots N_y\text{-}1 \;\; k: 0\ldots N_z \tag{610}$$

$$\mathrm{Ez}_{0,j,k}^{n+1} = \mathrm{Ez}_{1,j,k}^{n} + \mathrm{RC}_{0,j,k} \cdot \left[\mathrm{Ez}_{1,j,k}^{n+1} - \mathrm{Ez}_{0,j,k}^{n}\right] \quad j: 0\ldots N_y \;\; k: 0\ldots N_z\text{-}1 \tag{611}$$

Front face:

$$\mathrm{Ey}_{N_x,j,k}^{n+1} = \mathrm{Ey}_{N_x-1,j,k}^{n} + \mathrm{RC}_{N_x,j,k} \cdot \left[\mathrm{Ey}_{N_x-1,j,k}^{n+1} - \mathrm{Ey}_{N_x,j,k}^{n}\right] \quad j: 0\ldots N_y\text{-}1 \;\; k: 0\ldots N_z \tag{612}$$

$$\mathrm{Ez}_{N_x,j,k}^{n+1} = \mathrm{Ez}_{N_x-1,j,k}^{n} + \mathrm{RC}_{N_x,j,k} \cdot \left[\mathrm{Ez}_{N_x-1,j,k}^{n+1} - \mathrm{Ez}_{N_x,j,k}^{n}\right] \quad j: 0\ldots N_y \;\; k: 0\ldots N_z\text{-}1 \tag{613}$$

Left face:

$$\mathrm{Ex}_{i,0,k}^{n+1} = \mathrm{Ex}_{i,1,k}^{n} + \mathrm{RC}_{i,0,k} \cdot \left[\mathrm{Ex}_{i,1,k}^{n+1} - \mathrm{Ex}_{i,0,k}^{n}\right] \quad i: 0\ldots N_x\text{-}1 \;\; k: 0\ldots N_z \tag{614}$$

$$\mathrm{Ez}_{i,0,k}^{n+1} = \mathrm{Ez}_{i,1,k}^{n} + \mathrm{RC}_{i,0,k} \cdot \left[\mathrm{Ez}_{i,1,k}^{n+1} - \mathrm{Ez}_{i,0,k}^{n}\right] \quad i: 0\ldots N_y \;\; k: 0\ldots N_z\text{-}1 \tag{615}$$

Felix Meier
+41 44 867 3723
Roggenfarstrasse 31
www.felmeier.com
CH – 8193 Eglisau
felix.meier.45@bluewin.ch

Right face:

$$\mathrm{Ex}_{\mathrm{i,N_y,k}}^{\mathrm{n+1}} = \mathrm{Ex}_{\mathrm{i,N_y-1,k}}^{\mathrm{n}} + \mathrm{RC}_{i,\mathrm{N_y},k} \cdot \left[\mathrm{Ex}_{\mathrm{i,N_y-1,k}}^{\mathrm{n+1}} - \mathrm{Ex}_{\mathrm{i,N_y,k}}^{\mathrm{n}}\right] \qquad \text{i: 0…}N_x\text{-1 k: 0…}N_z \qquad (616)$$

$$\mathrm{Ez}_{\mathrm{i,N_y,k}}^{\mathrm{n+1}} = \mathrm{Ez}_{\mathrm{i,N_y-1,k}}^{\mathrm{n}} + \mathrm{RC}_{i,\mathrm{N_y},k} \cdot \left[\mathrm{Ez}_{\mathrm{i,N_y-1,k}}^{\mathrm{n+1}} - \mathrm{Ez}_{\mathrm{i,N_y,k}}^{\mathrm{n}}\right] \qquad \text{i: 0…}N_y \text{ k: 0…}N_z\text{-1} \qquad (617)$$

Bottom face:

$$\mathrm{Ex}_{\mathrm{i,j,0}}^{\mathrm{n+1}} = \mathrm{Ex}_{\mathrm{i,j,1}}^{\mathrm{n}} + \mathrm{RC}_{i,j,0} \cdot \left[\mathrm{Ex}_{\mathrm{i,j,1}}^{\mathrm{n+1}} - \mathrm{Ex}_{\mathrm{i,j,0}}^{\mathrm{n}}\right] \qquad \text{i: 0…}N_x\text{-1 j: 0…}N_y \qquad (618)$$

$$\mathrm{Ey}_{\mathrm{i,j,0}}^{\mathrm{n+1}} = \mathrm{Ey}_{\mathrm{i,j,1}}^{\mathrm{n}} + \mathrm{RC}_{i,j,0} \cdot \left[\mathrm{Ey}_{\mathrm{i,j,1}}^{\mathrm{n+1}} - \mathrm{Ey}_{\mathrm{i,j,0}}^{\mathrm{n}}\right] \qquad \text{i: 0…}N_x \text{ j: 0…}N_y\text{-1} \qquad (619)$$

Top face:

$$\mathrm{Ex}_{\mathrm{i,j,N_z}}^{\mathrm{n+1}} = \mathrm{Ex}_{\mathrm{i,j,N_z-1}}^{\mathrm{n}} + \mathrm{RC}_{i,j,\mathrm{N_z}} \cdot \left[\mathrm{Ex}_{\mathrm{i,j,N_z-1}}^{\mathrm{n+1}} - \mathrm{Ex}_{\mathrm{i,j,N_z}}^{\mathrm{n}}\right] \qquad \text{i: 0…}N_x\text{-1 j: 0…}N_y \qquad (620)$$

$$\mathrm{Ey}_{\mathrm{i,j,N_z}}^{\mathrm{n+1}} = \mathrm{Ey}_{\mathrm{i,j,N_z-1}}^{\mathrm{n}} + \mathrm{RC}_{i,j,\mathrm{N_z}} \cdot \left[\mathrm{Ey}_{\mathrm{i,j,N_z-1}}^{\mathrm{n+1}} - \mathrm{Ey}_{\mathrm{i,j,N_z}}^{\mathrm{n}}\right] \qquad \text{i: 0…}N_x \text{ j: 0…}N_y\text{-1} \qquad (621)$$

For evaluating (610) to (621), we do need some values of the previous time step. So those values must be saved before the E field components are updated by means of (211) to (213).

Felix Meier
+41 44 867 3723
Roggenfarstrasse 31
www.felmeier.com
CH – 8193 Eglisau
felix.meier.45@bluewin.ch

2.8.2 Mei Fang Superabsorption

The Mei-Fang superabsorption technique [108] is actually not an ABC, but a method to improve the performance of various ABCs. It is supposed to provide a dramatic reduction of the numerical error caused by boundary reflection.

The method starts by computing the Mur ABC for the H field in the same way as for the E field:

$$\frac{1}{2}\cdot\left[\frac{\mathrm{Hz}_{0,j,k}^{n+1}-\mathrm{Hz}_{0,j,k}^{n}}{\Delta t}+\frac{\mathrm{Hz}_{1,j,k}^{n+1}-\mathrm{Hz}_{1,j,k}^{n}}{\Delta t}\right]-\mathrm{v}_{\mathrm{rear}}\cdot\frac{1}{2}\cdot\left[\frac{\mathrm{Hz}_{1,j,k}^{n+1}-\mathrm{Hz}_{0,j,k}^{n+1}}{\Delta}+\frac{\mathrm{Hz}_{1,j,k}^{n}-\mathrm{Hz}_{0,j,k}^{n}}{\Delta}\right]=0 \qquad (622)$$

Again, after some manipulations, we get

$$\mathrm{Hz}_{0,j,k}^{n+1}=\mathrm{Hz}_{1,j,k}^{n}+\frac{\mathrm{v}_{\mathrm{rear}}\cdot\Delta t-\Delta}{\mathrm{v}_{\mathrm{rear}}\cdot\Delta t+\Delta}\cdot\left[\mathrm{Hz}_{1,j,k}^{n+1}-\mathrm{Hz}_{0,j,k}^{n}\right] \qquad (623)$$

Then, for obtaining the final value of $\mathrm{Hz}_{0,j,k}^{n+1}$, a weighted average is taken of the value as per (623) and of the value as computed by the regular update equation.

We define one more coefficient in order to simplify the notation in the update equations:

$$\mathrm{RC}=\frac{\mathrm{v}\cdot\Delta t-\Delta}{\mathrm{v}\cdot\Delta t+\Delta} \qquad (624)$$

And the ratio of the distance covered with one time step to the cell edge size is

$$\mathrm{Rho}=\rho=\frac{\mathrm{v}\cdot\Delta t}{\Delta} \qquad (625)$$

The update equations are

Rear face:

$$\mathrm{Hy}_{0,j,k}^{n+1}=\frac{1}{1+\rho}\left[\!\left[\mathrm{Hy}_{0,j,k}^{n+1}+\rho\cdot\left\{\mathrm{Hy}_{1,j,k}^{n}+\mathrm{RC}_{0,j,k}\cdot\left[\mathrm{Hy}_{1,j,k}^{n+1}-\mathrm{Hy}_{0,j,k}^{n}\right]\right\}\right]\!\right]$$

j: 0…N_y-1 k: 0…N_z (626)

$$\mathrm{Hz}_{0,j,k}^{n+1}=\frac{1}{1+\rho}\left[\!\left[\mathrm{Hz}_{0,j,k}^{n+1}+\rho\cdot\left\{\mathrm{Hz}_{1,j,k}^{n}+\mathrm{RC}_{0,j,k}\cdot\left[\mathrm{Hz}_{1,j,k}^{n+1}-\mathrm{Hz}_{0,j,k}^{n}\right]\right\}\right]\!\right]$$

j: 0…N_y k: 0…N_z-1 (627)

Front face:

$$\mathrm{Hy}_{N_x-1,j,k}^{n+1}=\frac{1}{1+\rho}\left[\!\left[\mathrm{Hy}_{N_x-1,j,k}^{n+1}+\rho\cdot\left\{\mathrm{Hy}_{N_x-2,j,k}^{n}+\mathrm{RC}_{N_x-1,j,k}\cdot\left[\mathrm{Hy}_{N_x-2,j,k}^{n+1}-\mathrm{Hy}_{N_x-1,j,k}^{n}\right]\right\}\right]\!\right]$$

j: 0…N_y-1 k: 0…N_z (628)

$$\mathrm{Hz}_{N_x-1,j,k}^{n+1}=\frac{1}{1+\rho}\left[\!\left[\mathrm{Hz}_{N_x-1,j,k}^{n+1}+\rho\cdot\left\{\mathrm{Hz}_{N_x-2,j,k}^{n}+\mathrm{RC}_{N_x-1,j,k}\cdot\left[\mathrm{Hz}_{N_x-2,j,k}^{n+1}-\mathrm{Hz}_{N_x-1,j,k}^{n}\right]\right\}\right]\!\right]$$

j: 0…N_y k: 0…N_z-1 (629)

Left face:

$$\mathrm{Hx}_{\mathrm{i,0,k}}^{\mathrm{n+1}} = \frac{1}{1+\rho}\left[\left[\mathrm{Hx}_{\mathrm{i,0,k}}^{\mathrm{n+1}} + \rho \cdot \left\{\mathrm{Hx}_{\mathrm{i,1,k}}^{\mathrm{n}} + \mathrm{RC}_{0,j,k} \cdot \left[\mathrm{Hx}_{\mathrm{i,1,k}}^{\mathrm{n+1}} - \mathrm{Hx}_{\mathrm{i,0,k}}^{\mathrm{n}}\right]\right\}\right]\right]$$

i: 0…N_x-1 k: 0…N_z (630)

$$\mathrm{Hz}_{\mathrm{i,0,k}}^{\mathrm{n+1}} = \frac{1}{1+\rho}\left[\left[\mathrm{Hz}_{\mathrm{i,0,k}}^{\mathrm{n+1}} + \rho \cdot \left\{\mathrm{Hz}_{\mathrm{i,1,k}}^{\mathrm{n}} + \mathrm{RC}_{0,j,k} \cdot \left[\mathrm{Hz}_{\mathrm{i,1,k}}^{\mathrm{n+1}} - \mathrm{Hz}_{\mathrm{i,0,k}}^{\mathrm{n}}\right]\right\}\right]\right]$$

i: 0…N_x k: 0…N_z-1 (631)

Right face:

$$\mathrm{Hx}_{\mathrm{i,N}_y-1,\mathrm{j,k}}^{\mathrm{n+1}} = \frac{1}{1+\rho}\left[\left[\begin{array}{c}\mathrm{Hx}_{\mathrm{i,N}_y-1,\mathrm{j,k}}^{\mathrm{n+1}} + \\ \rho \cdot \left\{\mathrm{Hx}_{\mathrm{i,N}_y-2,\mathrm{j,k}}^{\mathrm{n}} + \mathrm{RC}_{\mathrm{i,N}_y-1,\mathrm{j,k}} \cdot \left[\mathrm{Hx}_{\mathrm{i,N}_y-2,\mathrm{j,k}}^{\mathrm{n+1}} - \mathrm{Hx}_{\mathrm{i,N}_y-1,\mathrm{j,k}}^{\mathrm{n}}\right]\right\}\end{array}\right]\right]$$

i: 0…N_x-1 k: 0…N_z (632)

$$\mathrm{Hz}_{\mathrm{i,N}_y-1,\mathrm{j,k}}^{\mathrm{n+1}} = \frac{1}{1+\rho}\left[\left[\begin{array}{c}\mathrm{Hz}_{\mathrm{i,N}_y-1,\mathrm{j,k}}^{\mathrm{n+1}} + \\ \rho \cdot \left\{\mathrm{Hz}_{\mathrm{i,N}_y-2,\mathrm{j,k}}^{\mathrm{n}} + \mathrm{RC}_{\mathrm{i,N}_y-1,\mathrm{j,k}} \cdot \left[\mathrm{Hz}_{\mathrm{i,N}_y-2,\mathrm{j,k}}^{\mathrm{n+1}} - \mathrm{Hz}_{\mathrm{i,N}_y-1,\mathrm{j,k}}^{\mathrm{n}}\right]\right\}\end{array}\right]\right]$$

i: 0…N_x k: 0…N_z-1 (633)

Bottom face:

$$\mathrm{Hx}_{\mathrm{i,j,0}}^{\mathrm{n+1}} = \frac{1}{1+\rho}\left[\left[\mathrm{Hx}_{\mathrm{i,j,0}}^{\mathrm{n+1}} + \rho \cdot \left\{\mathrm{Hx}_{\mathrm{i,j,1}}^{\mathrm{n}} + \mathrm{RC}_{\mathrm{i,j,0}} \cdot \left[\mathrm{Hx}_{\mathrm{i,j,1}}^{\mathrm{n+1}} - \mathrm{Hx}_{\mathrm{i,j,0}}^{\mathrm{n}}\right]\right\}\right]\right]$$

i: 0…N_x-1 j: 0…N_y (634)

$$\mathrm{Hy}_{\mathrm{i,j,0}}^{\mathrm{n+1}} = \frac{1}{1+\rho}\left[\left[\mathrm{Hy}_{\mathrm{i,j,0}}^{\mathrm{n+1}} + \rho \cdot \left\{\mathrm{Hy}_{\mathrm{i,j,1}}^{\mathrm{n}} + \mathrm{RC}_{\mathrm{i,j,0}} \cdot \left[\mathrm{Hy}_{\mathrm{i,j,1}}^{\mathrm{n+1}} - \mathrm{Hy}_{\mathrm{i,j,0}}^{\mathrm{n}}\right]\right\}\right]\right]$$

i: 0…N_x j: 0…N_y-1 (635)

Top face:

$$\mathrm{Hx}_{\mathrm{i,j,N_z-1}}^{\mathrm{n+1}} = \frac{1}{1+\rho}\left[\left[\mathrm{Hx}_{\mathrm{i,j,N_z-1}}^{\mathrm{n+1}} + \rho \cdot \left\{\mathrm{Hx}_{\mathrm{i,j,N_z-2}}^{\mathrm{n}} + \mathrm{RC}_{\mathrm{i,j,N_z-1}} \cdot \left[\mathrm{Hx}_{\mathrm{i,j,N_z-2}}^{\mathrm{n+1}} - \mathrm{Hx}_{\mathrm{i,j,N_z-1}}^{\mathrm{n}}\right]\right\}\right]\right]$$

i: 0…N_x-1 j: 0…N_y (636)

$$\mathrm{Hy}_{\mathrm{i,j,N_z-1}}^{\mathrm{n+1}} = \frac{1}{1+\rho}\left[\left[\mathrm{Hy}_{\mathrm{i,j,N_z-1}}^{\mathrm{n+1}} + \rho \cdot \left\{\mathrm{Hy}_{\mathrm{i,j,N_z-2}}^{\mathrm{n}} + \mathrm{RC}_{\mathrm{i,j,N_z-1}} \cdot \left[\mathrm{Hy}_{\mathrm{i,j,N_z-2}}^{\mathrm{n+1}} - \mathrm{Hy}_{\mathrm{i,j,N_z-1}}^{\mathrm{n}}\right]\right\}\right]\right]$$

i: 0…N_x j: 0…N_y-1 (637)

Felix Meier
+41 44 867 3723
Roggenfarstrasse 31
www.felmeier.com
CH – 8193 Eglisau
felix.meier.45@bluewin.ch

2.8.3 Time Steps

Obviously, the ABC equations need not to be calculated before the wavefront reaches a face. To make sure we are on the safe side, we assume air only as a medium and we also assume that only the position of the signal source on the z axis will matter.

Let d be the shortest distance from the signal source to either the top or the bottom of the space. Then the first face will be reached after

$$\mathrm{ABCSteps} = \frac{\mathrm{d}}{\Delta} \tag{638}$$

time steps. So this is when the saving of previous face values and the evaluation of the ABC equations must be started.

2.8.4 Coefficients

The reflection coefficients $\frac{v \cdot \Delta t - \Delta}{v \cdot \Delta t + \Delta}$ will be the same for the rear, front, left and right faces since all layer interfaces are in the x-y plane, and the material properties are the same within the entire layer, so we can use a one-dimensional array for providing those coefficients. For the bottom and top faces, a single value will do for the same reason.

The same argument applies to the Rho coefficients.

3 Implementation

3.1 Indexing

We use zero based indexing as usual in C and C++: Array indexes start at 0 and go to N-1 for a N-dimensional array. Note that Matlab array indexes start at 1!

Since the C++ operator `new TYPE[]` does not accept multidimensional matrices, we assign the Yee cell data space as a one-dimensional vector and use the following indexing scheme:

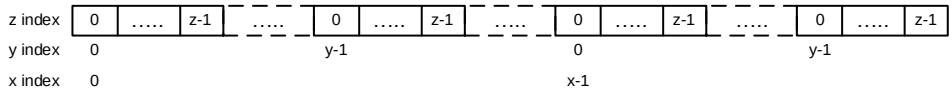

For the x dimension, the pointer to a Yee cell must be incremented or decremented by $(y \cdot z)$, and for the y dimension the pointer to a Yee cell must be incremented or decremented by z. The total size of the vector will then be $(x \cdot y \cdot z)$.

3.2 Arrays

3.2.1 The Project Space

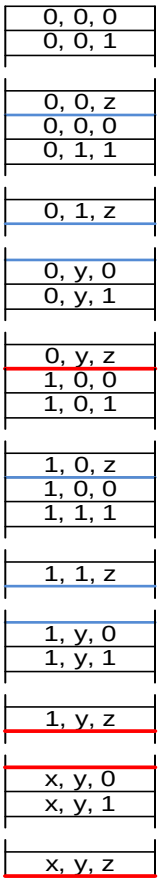

The project space is made of a three-dimensional grid of Yee cells. Since the E field vectors are located on the edges of the cells, we need an extra cell in every dimension for the E field vectors on the front, right and top faces of the project space. So the number of cells in the array will be `XCells+1`, `YCells+1` and `ZCells+1`, and the array indexes will go from `0` to `XCells`, `0` to `YCells` and `0` to `ZCells`.

Looping through all cells with the following code

```
for (i = 0; i <= XCells; i++)
{
  for (j = 0; j <= YCells; j++)
  {
    for (k = 0; k <= ZCells; k++)
    {
      …
    }
  }
}
```

can be implemented by just incrementing a pointer to a cell.

For walking through this array, we must use individual pointer increments $\mathrm{ndx} = (\mathrm{ny}+1) \cdot (\mathrm{nz}+1)$ and $\mathrm{ndy} = (\mathrm{nz}+1)$.

3.2.2 The Coefficients

Since all layer interfaces are in the x-y plane, and material properties are assumed to be homogenous and isotropic within every layer, we can use a one-dimensional array of size `ZCells+1` for all coefficients that depend on the material properties. For clarity, we will use two arrays, one for the coefficients for the update equations and another one for the coefficients for the ABC equations.

3.2.3 The Individual Faces

For the evaluation of the ABC equations, we do need E and H field values from the previous time step. Keeping a copy of the main cell array would take a very large amount of precious memory and a lot of time for saving the entire array, so we only save the contents of the outermost two cells for the rear, left and bottom faces and the outermost three cells for the front, right and top faces (since the H field vectors are located at the center of the face cells !) in six separate arrays. For the rear, left and bottom arrays, the indexing is as follows:

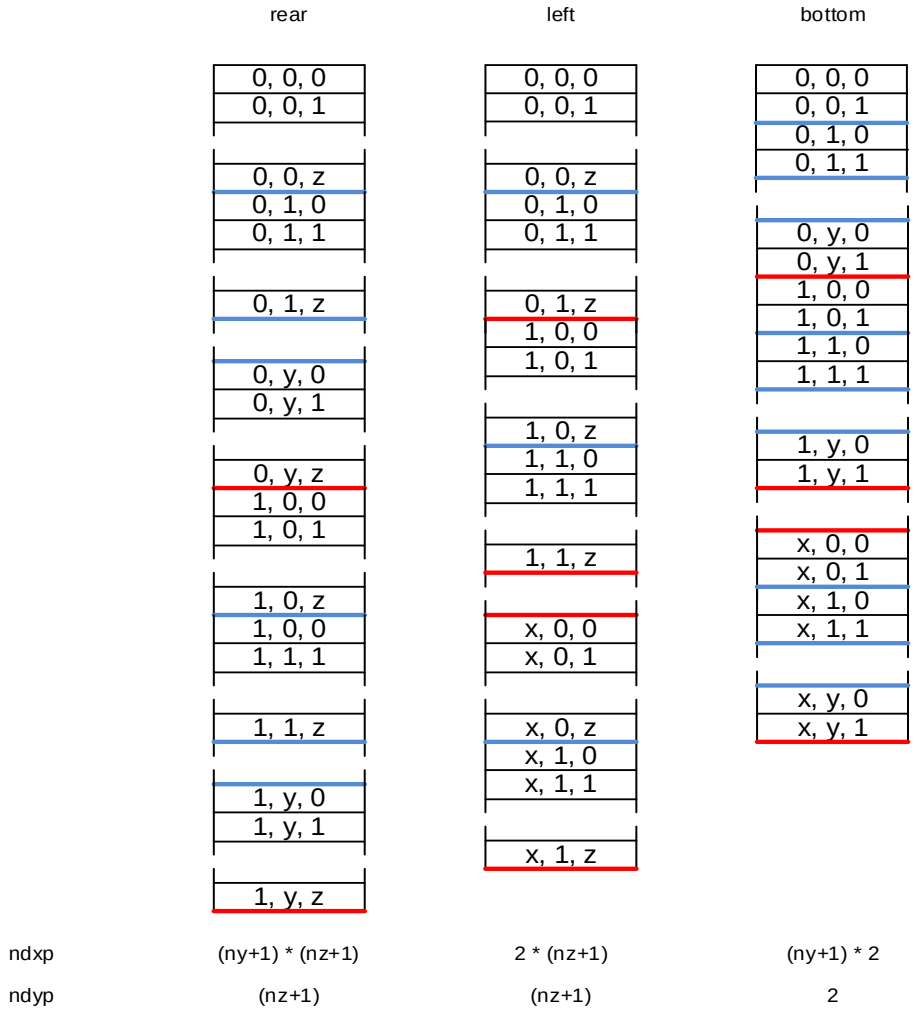

For walking through these arrays, we must use individual pointer increments `ndxp` and `ndyp` as shown for the x and y pointers.

For the front, right and top arrays, the indexing is as follows:

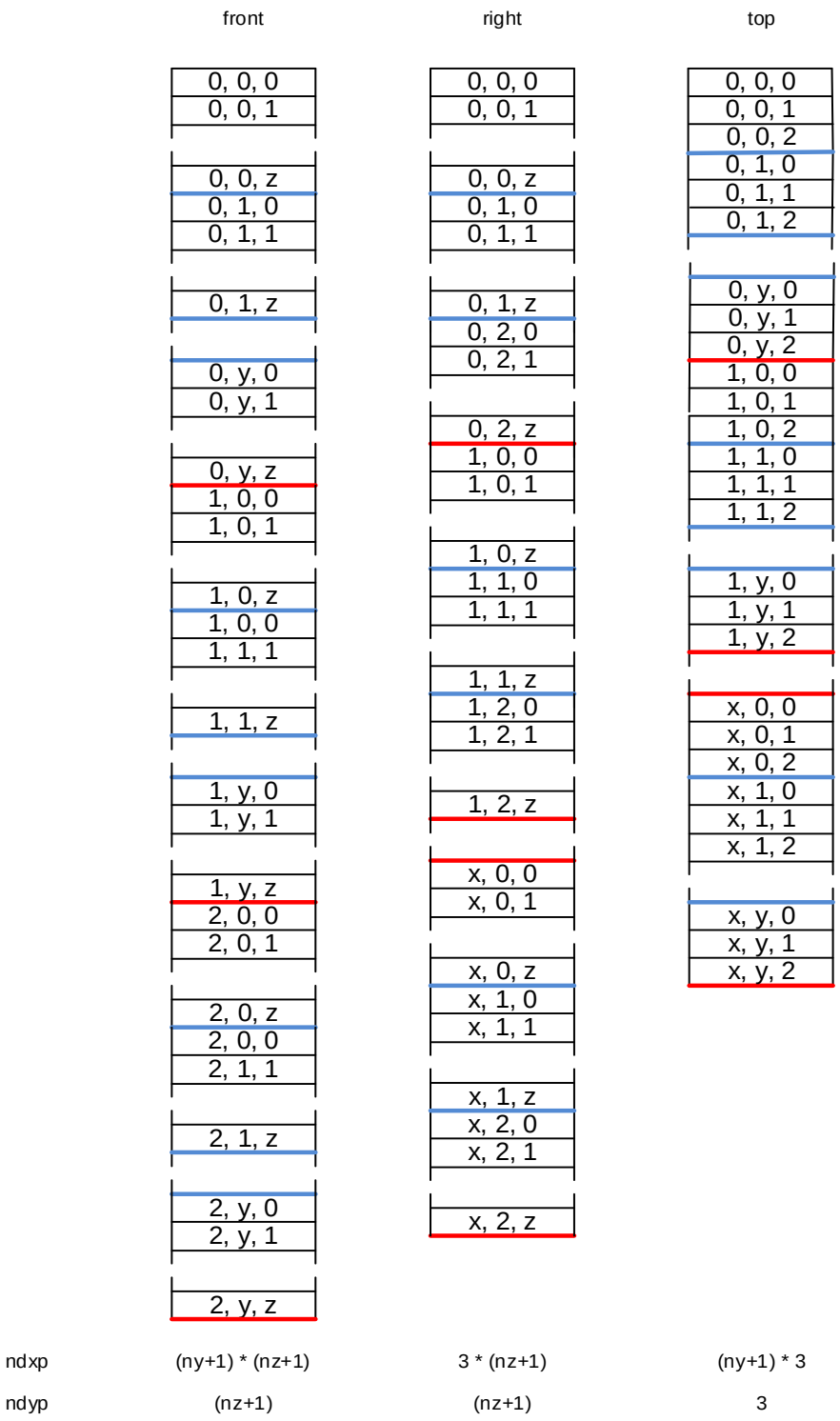

For walking through these arrays, we must use individual pointer increments ndxp and ndyp as shown for the x and y pointers.

4 Algorithm Validation

The FDTD Algorithm software has been validated by comparing the results with the results from a closed form solution of the dipole field in a homogenous space (free air).

Mc Tavish [401] has given the following equation for the field lines in Cartesian coordinates:

$$\frac{dy}{dx} = \frac{2 \cdot y^2 - x^2}{3 \cdot x \cdot y} \tag{700}$$

In the above formula, the y axis corresponds to the dipole axis, so, for our coordinate system, we have

$$\frac{dy}{dx} = \frac{3 \cdot x \cdot y}{2 \cdot x^2 - y^2} \tag{701}$$

The best match is achieved at about 600 to 700 iterations:

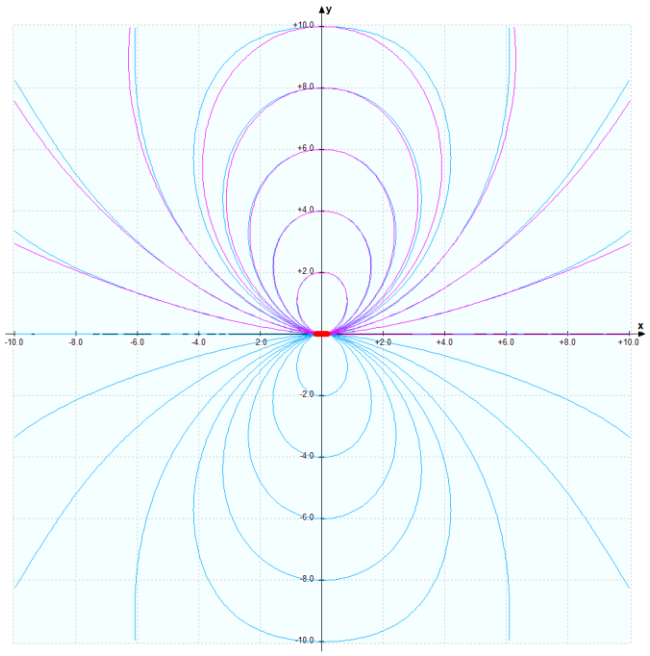

The magenta field lines in the upper half plane are field lines that have been calculated by the formula (701). The deviations are mostly caused by reflections at the faces. Some deviations may also be due to differences in the dipole dimensions: for the closed form formula, the dipole diameter and length are 0, whereas for the FDTD algorithm, the dipole diameter and length are both one Yee cell size, i.e. 10 cm in our default case.

If the number of iterations is lower, the numerical values calculated by means of the FDTD algorithm are not good enough yet, and with a higher number of iterations, the effects of reflections at the faces become more important.

When the field lines for a space of 40 meters by 40 meters are calculated, the resulting curves also compare well to the ones given by Ayuso in [400].

5 Optimization

The program was initially prepared with an emphasis on clarity, precision and ease of debugging. Once it ran correctly, several optimizations were applied. As a result, execution time was reduced by a factor of 4.4, and memory usage by a factor of 2.

5.1 Parallel Threads

On CPUs with four or more cores, the FDTD algorithm calculation is split up into two partitions and each partition is run on a separate core in parallel. This has quite an impact on total CPU usage:

Single Partition for FDTD

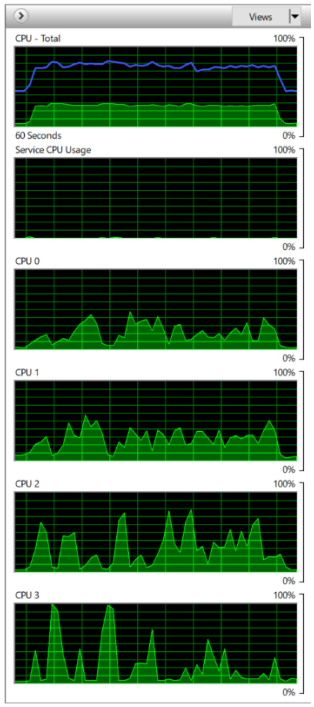

Two Partitions for FDTD

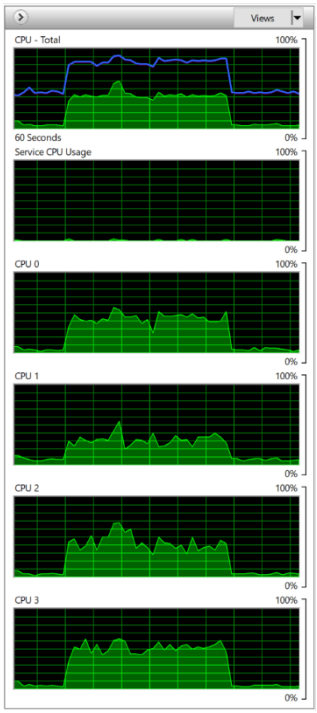

5.2 Loop Fusion

Originally, there were three triple loops for updating each of the E- and H-field components. After some preliminary processing, it became possible to combine the three loops to a single triple loop. This eliminated a lot of loop control overhead.

5.3 Localization of Variables

Variables residing in main memory and being accessed multiple times within a function are copied to auto variables that reside on the stack. The stack is very likely to reside in cache memory, so this saves a lot of time for memory access.

5.4 Inlining of Functions

Calls to small functions within the main loops were changed to inline code, thus eliminating the function call overhead.

5.5 Data Format

Originally, the data type used for the E- and H-field variables was `double`. Changing to the `float` type reduced memory requirements by a factor of 2 and also resulted in a substantial reduction of execution time since it requires less access to main memory.

6 Resources

6.1 Memory

The main array with all the E and H field values for every cell holds ((XCells+1) x (YCells+1) x (ZCells+1)) cells. Each field value takes 4 bytes at `float` precision, and there are 6 field values. Add some bytes for the storage of the previous values on the face layers. So this is an estimate of memory that should be available to the application without swapping to a hard disk.

X Cells	Y Cells	Z Cells	~Bytes
21	21	21	256'000
201	201	101	100'000'000
401	401	201	800'000'000

6.2 Computing Power

The calculation for a space of 201 by 201 by 101 cells takes 300 to 800 steps depending on the layer properties and results in a calculation time of about 30 seconds on an Intel® Xeon® W-2102 CPU with a clock frequency of 2.9 GHz.

6.3 Display

The vertical number of pixels of the display must be at least 1080.

6.4 Operating System

The application has been tested on computers running under Windows 7 and Windows 10.

6.5 Tools

The application was built using Microsoft Visual Studio Community Edition and the Microsoft Foundation Classes. The programming language is C++.

Felix Meier
+41 44 867 3723
Roggenfarstrasse 31
www.felmeier.com
CH – 8193 Eglisau
felix.meier.45@bluewin.ch

7 Layer Properties

The individual layers exhibit different electromagnetic properties:

7.1 Dielectric Permittivity

The dielectric permittivity is expressed as a product of the free space permittivity ε_0 and the relative permittivity ε_r:

$$\varepsilon = \varepsilon_0 \cdot \varepsilon_r$$

The permittivity ε_0 of free space is $8.854 \cdot 10^{-12}$ As/Vm. The relative permittivity ε_r of free space is 1.0.

The total dielectric permittivity is made of two components: The AC permittivity and the DC permittivity.

7.1.1 Dielectric Relaxation

The dielectric relaxation is dependent on the frequency. It is representing energy storage.

According to the Debye model, the dielectric relaxation results in a complex dielectric permittivity:

$$\varepsilon_r = \varepsilon_\infty + \frac{\varepsilon_s - \varepsilon_\infty}{1+\omega^2\tau^2} - j\frac{\varepsilon_s - \varepsilon_\infty}{1+\omega^2\tau^2} \cdot \omega\tau \;=\; \varepsilon_\infty + \frac{\varepsilon_s - \varepsilon_\infty}{1+j\omega\tau}$$

$$\varepsilon_r = \varepsilon' - j\varepsilon''$$

$$\varepsilon' = \varepsilon_\infty + \frac{\varepsilon_s - \varepsilon_\infty}{1+\omega^2\tau^2}$$

$$\varepsilon'' = \frac{\varepsilon_s - \varepsilon_\infty}{1+\omega^2\tau^2} \cdot \omega\tau$$

where

ε_s	static or low frequency permittivity
ε_∞	high frequency permittivity
$\tau = \tau_{AC}$	AC conductivity (frequency dependent)
ε_r	relative permeability
ω	angular frequency, $\omega = 2 \cdot \pi \cdot f$

Since the AC conductivity determines the imaginary part of ε_r, the formula for ε_r can be re-written

$$\varepsilon_r = \varepsilon_\infty + \frac{Re(\sigma_{AC})}{\omega\varepsilon_0} - j\frac{Im(\sigma_{AC})}{\omega\varepsilon_0}$$

7.1.2 Conductivity Relaxation

The conductivity relaxation is due to the DC conductivity of the material. It is representing energy loss. It adds another term to the imaginary part of the complex dielectric permittivity:

$$\frac{\sigma_{DC}}{\omega\varepsilon_0}$$

7.1.3 Total Permittivity

The total permittivity is composed of the permittivity that is caused by dielectric relaxation and of the permittivity that is caused by conductivity relaxation:

$\varepsilon_r = \varepsilon' - j\left(\varepsilon'' + \frac{\sigma_{DC}}{\omega\varepsilon_0}\right)$ or, since $\varepsilon' = \varepsilon_\infty + \frac{Re(\sigma_{AC})}{\omega\varepsilon_0}$ and $\varepsilon'' = \frac{Im(\sigma_{AC})}{\omega\varepsilon_0}$ [7], [8]

$$\varepsilon_r = \varepsilon_\infty + \frac{Re(\sigma_{AC})}{\omega\varepsilon_0} - j\left(\frac{Im(\sigma_{AC})}{\omega\varepsilon_0} + \frac{\sigma_{DC}}{\omega\varepsilon_0}\right)$$

Using complex values for ξ_r in the calculations would cause a heavy overhead. We therefore use real values for ξ_r only.

7.2 Magnetic Permeability

The magnetic permeability is expressed as a product of the free space permeability μ_0 and the relative permeability μ_r:

$$\mu = \mu_0 \cdot \mu_r$$

The permeability μ_0 of free space is $4\pi \cdot 10^{-7}$ Vs/Am. The relative permeability μ_r of free space is 1.0

There is almost no literature on the magnetic permeability of snow or soil. If so, it covers frequencies above 100 MHz that are used in satellite monitoring of the earth surface, so it is of no use to the subject of avalanche transceivers operating at 457 kHz.

For the purposes of visualizing the magnetic field produced by an avalanche transceiver, we therefore use a relative permeability of 1.0.

7.3 Electrical Conductivity

The electrical conductivity is a parameter representing the ability of a medium to conduct electrical currents. The unit of measurement is S/m (Siemens per meter) which is equal to 1/(Ω•m). The symbol used to stand for the conductivity is the Greek letter σ.

The electrical conductivity of snow is mostly caused by impurities such as salts that have been washed out of the atmosphere by precipitation.

7.4 Magnetic Conductivity

Since there is no such thing as a magnetic charge, there is no magnetic current. However, in metallic or ferromagnetic materials, there may be a frequency dependent loss due to eddy currents or rotation of magnetic moments.

Since the materials under consideration are not very conductive nor ferromagnetic, the equivalent magnetic loss σ_m is 1.0.

Felix Meier
+41 44 867 3723
Roggenfarstrasse 31
www.felmeier.com
CH – 8193 Eglisau
felix.meier.45@bluewin.ch

7.5 Numerical Values

7.5.1 Snow

7.5.1.1 Typical Values

for snow @ 457 kHz are:

Source	Type of Snow	ε_s	ε_∞	ε_r	τ_{AC}	σ_{AC}	σ_{DC}
Kuroiwa [212]	soft 0.10 g/m^3	3.1	1.2			2.0e-5	
	0.13 g/m^3	4.8	1.3				
	0.25 g/m^3	9.5	1.5				
	wet	26.0	4.0			6.4e-5	
	pure (hoar frost)	6.5	1.5			5.0e-6	
	granular	15.0	2.0			2.5e-5	
	compact	15.0	2.0			3.3e-5	
Evans [211]	soft new 0.13 g/m^3			4.0		1.0e-9	
	granular 0.40 g/m^3			15.0		1.0e-7	
	compact wet			50.0		1.0e-6	
Takei [220]	snow 0.40 g/m^3	20.0	1.8			4.0e-5	4.0e-7
	hoar-frost 0.39 g/m^3	16.0	1.8			1.7e-5	3.0e-8
Denoth [26]	low density recrystallized	38.5	3.15		2.03e-5		
	medium density, old, rounded crystals	13.5	1.51		1.82e-5		
Yosida [214]	newly fallen 0.10 g/m^3	3.0	1.2				
	newly fallen 0.25 g/m^3	9.5	1.5				
	wet 0.38 g/m^3 ,-2º	32.0	3.5				
	compact 0.40 g/m^3 ,-3º	13.5	2.0				
	granular 0.41 g/m^3 ,-4º	13.5	2.1				
	pure artificial hoar 0.29 g/m^3 ,-8.5º	6.5	1.6		1.85e-5		
Achammer [217]	old 0.43 g/m^3		3.0			2.5e-5	
Ayuso [200]	mildly wet			4.0 to 8.0		1.0e-6	1.0e-6

7.5.1.2 Simulation values

snow type	ε_∞	σ_{AC}	μ_r
pure (fresh)	1.5	5e-6	1.0
wet	3.5	5e-5	1.0
default (typical)	2.0	1e-5	1.0

Since σ_{AC} apparently is considerably higher than σ_{DC}, it will dominate the value of the imaginary part of ε_r.

On the Cole diagram, we are at a point to the very left of the semi-circle.

$\frac{Re(\sigma_{AC})}{\omega\varepsilon_0}$ is very small and can be neglected for snow.

$\frac{\sigma_{AC}}{\omega\varepsilon_0}$ is almost equivalent to $\frac{Im(\sigma_{AC})}{\omega\varepsilon_0}$.

So all we need to consider is $\varepsilon_r = \varepsilon_\infty - j\frac{\sigma_{AC}}{\omega\varepsilon_0}$.

7.5.2 Soil

7.5.2.1 Typical Values

for snow @ 457 kHz are:

Source	Ref.	Type of Soil	ε_s	ε_∞	ε_r	τ_{AC}	σ_{AC}	σ_{DC}
Evans	[211]	dry sand or rock	10.0	2.0	8.0		1.0e-4 1.0e-5	
Fano	[310]	dry sand			3.0		1.0e-4 1.0e-5	
		humid sand			20.0		1.0e-2	
		dry earth			7.0		1.0e-4 1.0e-5	
ITU	[301]	very dry ground			3.0		1.0e-4	
		medium dry ground			15.0		1.0e-3	
		wet ground			30.0		1.0e-2	
Grisso	[320]							1.0e-3 1.0e-2
Ayuso	[201]	Soil			8.0			1.0e-3

According to Ayuso, the effective conductivity of soil is dominated by the bulk DC conductivity.

7.5.2.2 Simulation values

soil type	ε_∞	σ_{AC}	μ_r
dry	8.0	1e-4	1.0
default (typical)	8.0	1e-4	1.0

8 References

8.1 The FDTD Algorithm

[100] Taflove, A., Hagness, S. C., M. E.; Computational Electrodynamics, The Finite Difference Time Domain Method; 3rd Edition, Artech House Inc. 2005

[101] Taflove, A., Brodwin, M. E.; Numerical Solution of Steady-State Electromagnetic Scattering Problems Using the Time-Dependent Maxwell's Equations; IEEE Trans. on MTT, August 1975, pp. 623 – 630.

[102] Yee, K.S..; Numerical Solution of Initial Boundary Value Problems Involving Maxwell's Equations in Isotropic Media; IEEE Trans. On Antennas and Propagation, Vol. 14, No. 3, May 1966, pp. 302 - 307.

[103] Mur, G.; Absorbing Boundary Conditions for the Finite-Difference Approximation of the Time-Domain Electromagnetic-Field Equations; IEEE Trans. EMC, Vol. EMC-23, No. 4, November 1981, pp. 377 - 382.

[104] Courant, R.; Friedrichs, K.; Lewy, H. (March 1967) [1928], "On the partial difference equations of mathematical physics", IBM Journal of Research and Development **11** (2): 215–234.

R. Courant, K. Friedrichs, and H. Lewy. "Uber die partiellen Differenzengleichungen der mathematischen Physik"; Mathematische Annalen, 100(1):32-74, 1928

[105] Schild, S. Advanced Material Modeling in EM-FDTD; PhD Dissertation, ETH Zürich, 2008.

[106] A 3D FDTD Code Implemented in MATLAB; Neva Electromagnetics; 2011

[107] Schneider, John B.; Understanding the Finite-Difference Time-Domain Method; August 18, 2020; https://eecs.wsu.edu/~schneidj/ufdtd/ufdtd.pdf

[108] Mei, K. K. and Fang, J.; Superabsorption – A Method to Improve Absorbing Boundary Conditions; IEEE Trans. Antennas and Propagation, Vol. 40, No. 9, Sep. 1992, pp. 1001- 1010.

[109] Mur, G.; Total-Field Absorbing Boundary Conditions for the Time-Domain Electromagnetic Field Equations; IEEE Trans. On Electromagnetic Compatibility, Vol. 40, No. 2, May 1998, pp 100 - 102.

8.2 Layer Properties

8.2.1 Snow

[200] Ayuso, Cuchi, J.A., N., Lera, F., Villarroel, J.L.; Avalanche Beacon Magnetic Field Calculations for Rescue Techniques Improvement; in: 2007 IEEE International Geoscience and Remote Sensing Symposium, pp. 722-725, 2007.

8.2.1.1 Permittivity

[210] Cole, K.S., Cole, R.H.; Dispersion and Absorption in Dielectrics; J. of Chemical Physics, Vol. 9, April 1941, pp. 341-351

[211] Evans, S.; Dielectric Properties of Ice and Snow – A Review; J. Glaciol. 5, 773–792 (1965)

[212] Kuroiwa, K.; The Dielectric Property of Snow; Proc. IGU, Rome (1954).

[213] Stiles, W.H., Ulaby, F.T.; Dielectric Properties of Snow; Remote Sensing Laboratory Tech. Report 527-1, University of Kansas Center for Research, Inc., Lawrence, KS, 1981

[214] YOSIDA, Zyungo; OURA, Hirobumi; KUROIWA, Daisuke; HUZIOKA, Tosio; KOJIMA, Kenji; KINOSITA, Seiiti; Physical Studies on Deposited Snow. Ⅴ. ; Dielectric Properties; Contributions from the Institute of Low Temperature Science, 14: 1-33, 1958

[215] Frübing, P.; Dielectric Spectroscopy; University of Potsdam, Institute of Physics, Advanced Lab Experiments, section M6; May 31, 2001

[216] Denoth, A.; Static Dielectric Constant as a Textural Index of Snow; Annals of Glaciology, Vol. 6, 1985, pp. 203-206

[217] Achammer, T., Denoth, A., 1994. Snow dielectric properties: from dc to microwave x-band. Annals of Glaciology 19, 92-96.

8.2.1.2 Conductivity

[220] Takei, I., Norikazu, M.; The Low Frequency Conductivity of Snow Near the Melting Temperature; Annals of Glaciology, 32 2001, pp 14-18.

8.2.2 Soil

[300] Liu, Ning; Soil and site characterization using electromagnetic waves; Thesis (Ph.D.)—Virginia Polytechnic Institute and State University, 2007, Chapter 2.

[301] Electrical Characteristics of the Surface of the Earth; ITU Recommendation ITU-R P.527-3, 1992.

[302] Scott, J.H.; Electrical and Magnetic Properties of Rock and Soil; United States Department of the Interior, Geological Survey; Open-File Report 83-915, 1983.

8.2.2.1 Permittivity

[310] Fano, W. G. and V. Trainotti; Dielectric properties of soils; IEEE Conference on Electrical Insulation and Dielectric Phenomena, 75–78, 2001.

8.2.2.2 Conductivity

[320] Grisso, R. et al.; Soil Electrical Conductivity; Virginia Cooperative Extension, Publication 442-508.

8.3 Others

[400] Ayuso, N., Cuchí, J.A., Lera, F., Villaroel J.L.; A deep insight into avalanche transceivers for optimizing rescue; Cold Region Science and Technology, Vol. 111 (2015), pp. 80-94.

[401] Mc Tavish, J. P.; Field pattern of a magnetic dipole; Am. J. Phys. Vol. 68, No. 6, June 2000; pg. 577-578